

Theory of Mechanical Properties of Ceramic-Matrix Composites

William A. Curtin

BP Research, Cleveland, Ohio 44128

A theory is presented to predict the pullout work and ultimate tensile strength of ceramic-matrix composite (CMC) materials tested under uniaxial tension as functions of the underlying material properties. By assuming that the fibers fracture independently and that global load redistribution occurs upon fiber fracture, the successive fragmentation of each fiber in the multifiber composite becomes identical to that of a single fiber embedded in a homogeneous large-failure-strain matrix, which has recently been solved exactly by the present author. From single-fiber fragmentation, the multifiber composite distribution of pullout lengths, work of pullout, and ultimate tensile strength are easily obtained. The trends in these composite properties as a function of the statistical fiber strength, the fiber radius and fill fraction, and the sliding resistance τ between the fibers and the matrix easily emerge from this approach. All these properties are proportional to a characteristic gauge length δ_c and/or the associated characteristic stress σ_c , with proportionality constants depending only very weakly on the fiber Weibull modulus: the pullout lengths scale with δ_c , the work of pullout scales with $\sigma_c \delta_c$, and the ultimate strength scales with σ_c . The key length δ_c is the generalization of the "critical length," defined by Kelly for single-strength fibers, to fibers with a statistical distribution of strengths. The theory also provides an interpretation of fracture-mirror measurements of pulled-out fiber strengths so that the *in situ* key strength σ_c and Weibull modulus of the fibers can be determined directly. Comparisons of the theoretical predictions of the ultimate tensile strength to literature data on Nicalon/lithium aluminum silicate (LAS) composites generally show good agreement. [Key words: ceramics, composites, strength, pullout, toughness.]

I. Introduction

IT is now well established that ceramic materials can be toughened appreciably by the addition of strong, continuous fiber reinforcements.¹⁻³ A major portion of the toughness is attributable to the work required to pull broken fibers out of the matrix against a frictional sliding resistance τ between the fiber and matrix.^{4,5} The magnitude of the toughness depends on τ , the fiber radius r and volume fraction f , and the fiber strength statistics (Weibull modulus m and mean strength σ_0 at gauge length L_0). The fiber strength statistics are particularly important because they determine the stress and the location of fiber breaks relative to the ultimate crack plane and, hence, determine the pullout lengths and ultimate composite strength. However, substantial pullout occurs only if the fibers can survive the onset of matrix cracking, which occurs at a stress σ_{mc} also dependent on many system properties.^{2,3,5-9} The dependence of pullout on all the material

parameters has been studied, usually with a focus on events in the vicinity of a single matrix crack, and existing theories predict very complicated dependences on m , σ_0 , τ , and r .^{4,5} In this paper, we analyze the fiber pullout length distribution and its contributions to the work of fracture under conditions of multiple matrix cracking prior to composite failure. Within the same basic mechanics assumptions as Suteu⁴ and Thouless and Evans⁵ (to be discussed below), we calculate the pullout length distribution by recognizing, under these conditions, that, during the course of loading to failure, every fiber experiences a complete uniaxial tension test *identical* to that occurring in a hypothetical single-fiber composite tension test in a matrix with a large failure strain. In effect, all of the other sliding fibers collectively form an effective large-failure-strain matrix into which any single fiber is embedded. Each fiber thus ultimately breaks into a set of fragments, the length distribution $P(x)$ of which we have recently calculated exactly as a function of τ , m , σ_0 , L_0 , and r .⁹ The pullout properties of the composite can then be calculated easily from the known fiber fragment distribution. The maximum tensile strength of the composite is also found easily within this framework.

As noted above, an important determinant of composite behavior is the statistical fiber strength. The number and strength of various defects which occur along the fiber must be described statistically. Here, we take the cumulative number of defects which can fail at stress σ in a length L of fiber to be given by the well-known Weibull expression

$$\Phi(L, \sigma) = \frac{L}{L_0} (\sigma/\sigma_0)^m \quad (1)$$

Insight into the scale parameters L_0 and σ_0 is gained by recognizing that σ_0 is the stress required to cause one failure, on average, in a fiber of length L_0 . m describes the variability, or dispersion, of measured strengths about the average. The quantity Φ is related to the commonly measured probability of failure $P_f(L, \sigma)$ by

$$P_f(L, \sigma) = 1 - \exp(-\Phi(L, \sigma))$$

used to interpret strength data in ceramic materials.

The dependence of fiber strength on L exhibited in Eq. (1) implies that quoted fiber strengths must *always* be accompanied by the appropriate gauge length and Weibull modulus, so that the fiber strength at the gauge length of interest can be determined. In the single-fiber fragment problem, the fiber strength statistics determine a characteristic length δ_c for the fiber fragments. δ_c is defined as the sliding length at a characteristic stress σ_c , and $\delta_c = r\sigma_c/\tau$, and σ_c is itself the average strength of a length δ_c of fiber. The latter requirement implies that $\Phi(\delta_c, \sigma_c) = 1$, and, using Eq. (1) with $\delta_c = r\sigma_c/\tau$, yields

$$\delta_c = \left(\frac{\sigma_0 r L_0^{1/m}}{\tau} \right)^{m/(m+1)} \quad (2a)$$

as the characteristic length of the fragments. In the limit of single-strength fibers, i.e., $m = \infty$, the fragment distribution is identical to that described by Kelly: all fragments are between $l_c/2$ and l_c , with $l_c = r\sigma_0/\tau$ (the so-called critical length).¹ For $m \leq \infty$, δ_c is the relevant length and δ_c is identi-

D. B. Marshall—contributing editor

cal to l_c in the $m \rightarrow \infty$ limit. For ceramic-matrix composites (CMCs), the identification of the proper gauge length of fiber relevant to composite tensile failure is crucial. This relevant gauge length is not simply the composite length, but rather is determined by several material properties. If we consider that the CMC failure is a collection of single-fiber fragmentation processes, then the relevant gauge length for CMC failure is proportional to δ_c , and the relevant strength is σ_c , given by

$$\sigma_c = \left(\frac{\sigma_0^m \tau L_0}{r} \right)^{1/(m+1)} \quad (2b)$$

The composite ultimate strength is proportional to $f\sigma_c$, with an m -dependent proportionality constant which accounts for the bundlelike nature of the composite failure.

Fiber pullout in the composite also depends on the single-fiber fragment length distribution $P(x)$, which in turn scales with δ_c . Specifically, the pullout properties of the composite are proportional to various moments

$$\langle x^n \rangle = \int dx x^n P(x)$$

of $P(x)$, and $\langle x^n \rangle$ can be written as

$$\langle x^n \rangle = \lambda_n(m) \delta_c^n \quad (3)$$

where the $\lambda_n(m)$ are known functions of m only and vary slowly with m , so that the main dependence of pullout properties on the material parameters is through δ_c . Thus, the key indicators of uniaxial tensile composite performance after matrix cracking depend only on δ_c and/or σ_c .

As a preview, we highlight our main results here and show the ubiquitous appearance of the δ_c and σ_c . The mean pullout length is found to be

$$\langle L \rangle = \frac{1}{4} \frac{\langle x^2 \rangle}{\langle x \rangle} = \frac{1}{4} \frac{\lambda_2(m)}{\lambda_1(m)} \delta_c \quad (4)$$

The work of pullout per unit area is simply proportional to the second moment of the pullout length distribution, which in turn is proportional to $\langle x^3 \rangle / \langle x \rangle$ and, therefore, ultimately takes the form

$$W_p = \frac{1}{12} f \frac{\lambda_3(m)}{\lambda_1(m)} \sigma_c \delta_c \quad (5)$$

A good analytic estimate of the ultimate tensile strength (UTS) of the composite is

$$\sigma_u = f \sigma_c \left(\frac{2}{m+2} \right)^{1/(m+1)} \frac{m+1}{m+2} \quad (6)$$

These simple relations show that the dependence of $\langle L \rangle$, W_p , and σ_u on τ , r , and m is predominantly through the relevant gauge length δ_c and σ_c . Using Eq. (2) in Eqs. (4) and (5) yields exactly the complicated trends of $\langle L \rangle$ and W_p as functions of σ_0 , r , and τ predicted by Sutcu⁴ and by Thouless and Evans⁵ under conditions of single matrix crack formation, but with important differences in the m -dependent coefficients (λ_2/λ_1 and λ_3/λ_1). The shape of the pullout length distribution also differs somewhat from that of Sutcu and of Thouless and Evans. An analytic expression for σ_u including all contributions to the strength and consistent with the theory for pullout has not previously been put forth.

Within the framework of the present theory, the in situ fiber strength statistics σ_c and m at gauge lengths approximately equal to δ_c can also be determined precisely from fracture-mirror measurements of the strengths of the pulled-out fiber fragments. The use of fracture mirrors to obtain some estimate of in situ strengths has been introduced previously,^{10,11} but the single-fiber composite fragmentation theory allows for an improved, consistent interpretation of the fracture-mirror fiber strength data to obtain σ_c and m directly.

Unfortunately, only a small amount of complete data on CMCs exists in the literature. Comparison of the theory predictions to data are thus limited to comparisons of σ_u . Our result for σ_u , which is an upper bound, compares very well with the data of Prewo¹² but is higher than that measured by Cao *et al.*,^{11,13} both on Nicalon (Nippon Carbon Co., Tokyo, Japan)/glass matrix systems. In principle, the theory provides a clear guide for assessing trade-offs between ultimate strength and work of fracture and their dependences on the many system parameters.

The remainder of this paper is structured as follows. In Section II we describe our model of composite failure under tensile loading and show how the dependence on single-fiber composite fragmentation arises. From the fragmentation theory, we then calculate pullout lengths and work of fracture. Section III describes the calculation of the ultimate tensile strength. In Section IV we show how fracture-mirror data are related to the in situ parameters σ_c and m . Comparisons of theory and experiment are presented in Section V. Section VI contains further discussion and implications of this theory. The Appendix discusses the small contribution to the work of fracture associated with the actual fiber breakage.

II. Model of Composite Pullout

We consider a ceramic matrix of modulus E_m uniaxially reinforced with a volume fraction f of cylindrical fibers of radius r , modulus E_f , mean tensile strength σ_0 at reference length L_0 , and Weibull modulus m describing both the distribution of strengths about σ_0 and the scaling of strength with fiber length L (see Eq. (1)). Under uniaxial tension along the fiber axis, the response of the composite is linear with modulus $E = fE_f + (1-f)E_m$ until a critical matrix-cracking load σ_{mc} is applied. At σ_{mc} , small preexisting matrix cracks propagate across the sample. It is assumed that, rather than propagating through the fibers, the fiber-matrix interface debonds and sliding of the fibers relative to the matrix occurs with sliding resistance τ . Under these conditions, σ_{mc} has been calculated as³

$$\sigma_{mc} = \left(\frac{6\tau\Gamma_m}{r} \frac{f^2 E_f E^2}{(1-f)E_m^2} \right)^{1/3} \quad (7)$$

where Γ_m is the matrix fracture energy. After one matrix crack has propagated, the stress in the matrix builds up to the pre-cracked value $\sigma_{mc}^m = E_m \sigma_{mc} / E$ through stress transfer across the sliding fiber-matrix interface over a sliding length l_m . Within a shear-lag analysis, l_m is

$$l_m = r \sigma_{mc}^m / 2\tau \quad (8)$$

Farther away than $\pm l_m$ from the first matrix crack, the same conditions for matrix cracking prevail as in the absence of the first matrix crack. Thus, additional matrix cracks can propagate across the sample. Each matrix crack formed excludes a region $\pm l_m$ around it from subsequent matrix cracking, and, therefore, the matrix-cracking process ceases when no more regions of the matrix carry the load σ_{mc}^m required for matrix-crack formation. In principle this multiple matrix cracking may occur over a range of stress $\geq \sigma_{mc}$ because of the distribution of initial flaws in the matrix, but for simplicity we assume here that all the multiple matrix cracking occurs at σ_{mc} . As a consequence of the possibility of overlapping of the sliding lengths (l_m) of neighboring matrix cracks, the matrix crack spacings are distributed between a minimum of l_m and a maximum of $2l_m$, with a mean spacing of $1.337l_m$.^{9,14} Note that experimental measurements of σ_{mc} and the mean matrix crack spacing $1.337l_m$ provide two approaches to determining τ via Eqs. (7) and (8), since all other quantities in Eqs. (7) and (8) are, in principle, known a priori.

As a consequence of matrix cracking at σ_{mc} , the stresses on the fibers are increased all along their lengths, and, in particular, the fibers carry the entire applied load σ_{mc} at the

matrix-crack planes; therefore, the fiber stresses there are σ_{mc}/f . Figures 1(A) and (B) show the distribution of stress in the matrix and the fibers just prior to and just after matrix cracking. After matrix cracking, all subsequent loads applied to the system are carried by the fibers, since the stresses in the matrix cannot be further increased. Thus, at applied stresses $\sigma > \sigma_{mc}$ and in the absence of any fiber failure (see below), the maximum fiber stress is σ/f (at the matrix-crack planes), and the minimum fiber stress is $\sigma/f - [\sigma_{mc}(1-f)E_m/fE]$ as shown in Fig. 1(C).

Now consider the occurrence of a single break in one fiber, formed when the stress at some point along the fiber reaches the value at which a defect in the fiber at that point can propagate and fracture the fiber. The fiber stress drops to zero at the break, and, as in the case of matrix cracking, the stress in the fiber builds up through the stress transfer across the sliding fiber-matrix interface. The sliding length l_f required to build the fiber stress up to its previous uncracked value at length l_f is then

$$l_f = r\sigma_f(l_f)/2\tau \quad (9)$$

where $\sigma_f(l_f)$ is the fiber stress previously existing at l_f away from the break, and always satisfies $\sigma/f - [\sigma_{mc}(1-f) \cdot E_m/fE] \leq \sigma_f(l_f) \leq \sigma/f$ at externally applied stress σ (see Fig. 1(D)). Also, $\sigma_f(l_f) \geq (1-f)\sigma_{mc}/f$ so that values of l_f are almost always larger than l_m .

The stress dropped by the broken fiber is picked up by the remaining intact fibers since the matrix cannot support any additional loads. Intact—in the context of multiple fiber breaking—is defined as follows: An element of fiber length is "intact" if there are no breaks in the same fiber within l_f of that element; that element is then capable of carrying additional loads transferred to it by breaks in the other fibers. However, we do not know the precise manner in which the load stress transfer is accomplished. Here, we assume that the total stress on any plane perpendicular to the fiber direction is unchanged by load transfer and that the load dropped in any plane by fibers broken within $\pm l_f$ of that plane is shared

equally by all intact fiber elements in that plane. Specifically, consider a plane at distance z along the fiber axis. Fibers which have a break within $\pm l_f$ of the plane at distance z cannot carry the average load per fiber σ/f at z —their load-carrying capacity at z is limited by the presence of the nearby break. Since the total average fiber load at the plane at distance z must still be σ/f , the loads on all intact fibers (i.e., fibers with no breaks within $\pm l_f$ of the plane at distance z) must be higher than the average. Equal, or global, load sharing assumes that all these intact fibers carry the same enhanced load at the plane at distance z . This assumption is also made by Sutcu⁴ and by Thouless and Evans.⁵ As multiple breaks appear in the fibers throughout the composite, the average stress on the intact portions of fibers increases monotonically, although not uniformly, along the length of the composite. The stress profile along a partially fragmented fiber is shown in Fig. 2(A). A break in a fiber at point z occurs if the stress at z attains the required failure stress, by a combination of externally applied load and load transfer from broken fibers, before the point z is subsumed within the l_f of some other break along the same fiber.

To obtain the distribution of fiber break points, or equivalently the distribution of fragment lengths created in each fiber as the composite is stressed, we proceed as follows. First, we neglect the variations in axial fiber stress caused by the presence of the matrix cracks, as indicated in Fig. 2(B), by effectively setting $\sigma_{mc}^m = 0$. Since the magnitudes of these variations is $(1-f)\sigma_{mc}E_m/fE$, their neglect is valid in the limit that the typical fiber strengths on gauge lengths l_f are much greater than $(1-f)\sigma_{mc}E_m/fE$. This approximation also now allows us to proceed with investigating fiber fragmentation without regard to the actual locations of the matrix cracks. Second, now focusing on a single fiber, we neglect variations in the axial fiber stress in each intact region between the slip lengths l_f of neighboring breaks, and approximate the stress in these regions by the average stress, as shown in Fig. 2(C). Because the entire composite contains many fibers, the variations in stress along each intact region of a fiber are small; therefore, neglecting them and using the average is a reasonable approximation. Note that different intact regions along the same fiber can have different average stresses.

We can now predict the evolution of fiber breaks, and hence fiber fragment lengths, in each fiber. During the course of an entire tensile test of the composite, each fiber undergoes monotonic tensile loading in each of its intact regions from zero stress to the failure stress of the intact region and hence, breaks into smaller and smaller fragments. As the spatially constant applied stress in an intact region increases, the region either shrinks, because the l_f on either end increase, or breaks. If a break occurs, then either (i) two new intact re-

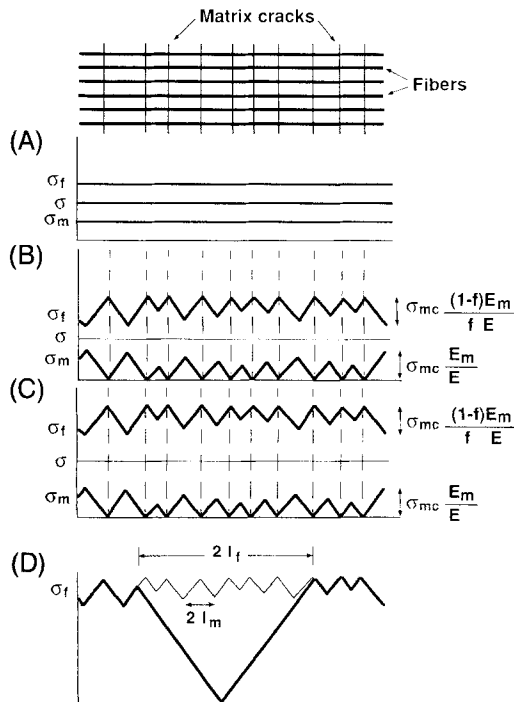


Fig. 1. Schematic of stress profiles in matrix (σ_m) and fiber (σ_f): (A) just prior to matrix cracking, (B) just after matrix cracking at applied stress σ_{mc} , (C) under further loading, $\sigma > \sigma_{mc}$, (D) fiber stress after a single break (light line shows stress prior to break) (note that the slip length l_f is longer than l_m).

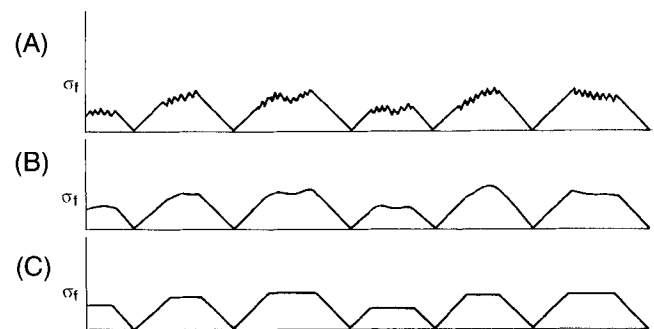


Fig. 2. Schematic of stress profile in fiber after partial fiber fragmentation: (A) true stress profile including variations due to matrix cracking, (B) approximate profile after neglecting matrix cracking but retaining variations due to load transfer from other fibers, and (C) approximate profile after averaging over stress variations in each intact region between fiber breaks. Evolution of the fiber fragmentation given in profile (C) is identical to that of a single-fiber composite tested in tension.

gions form on either side of the new break, (ii) one smaller intact region forms if the slip length of the new break overlaps one of the slip lengths on either side, or (iii) a “dead zone” forms if both the slip lengths of the new break intersect the slip lengths on either side, so that the entire intact region is taken up by the slip lengths. *This process of successive fiber fragmentation is precisely the same as the formation of fragment pieces during a full tensile test on a single-fiber composite (SFC) in a large strain-to-failure matrix. From the point of view of any one fiber, the remaining fibers and matrix form an effective large-failure-strain matrix into which that fiber is embedded.* The fact that different intact regions along a fiber may experience different average stress levels at some point in the multifilament composite is not important since, once a fiber breaks into two pieces, the subsequent fragmentation of each of the two remaining pieces does not depend on the presence of the other piece. *Therefore, at the end of the composite tensile test, each fiber in the composite has undergone, effectively, a single-fiber tensile test and the distribution of fiber fragments in each fiber is identical to the distribution of fragments in the SFC.* We have recently described a method to calculate the single-fiber fragment distribution exactly.⁹ Therefore, within the approximation described above and shown schematically in Fig. 2, the fiber fragment distribution $P(x)$ ($P(x) dx$ = fraction of fragments between $x, x + dx$) in the multifiber composite at the end of the tensile test is known exactly. *The characteristic length scale for these fragments at the end of a single-fiber test in a hypothetical nonfailing matrix is the length δ_c given in Eq. (2), which bears reproducing here:*

$$\delta_c = \left(\frac{\sigma_0 r L_0^{1/m}}{\tau} \right)^{m/(m+1)} \quad (2)$$

The cumulant of the single-fiber fragment probability distribution

$$F(x) = \int_0^x dx' P(x')$$

versus the normalized fragment length x/δ_c is shown in Fig. 3 (in Weibull form, $\ln[-\ln(1 - F)]$ vs $\ln(x/\delta_c)$) for a range of Weibull moduli.

To obtain the pullout length distribution $P(L)$ from the fragment distribution $P(x)$, we need to know the locations of the fiber breaks relative to the matrix cracks. However, since our determination of the fragment lengths was made independent of the matrix-crack locations, any chosen matrix crack intersects each fiber at a random position (see Fig. 4). The probability of intersecting a fragment of length x , $P_i(x)$, is proportional to the length x and the probability of occurrence

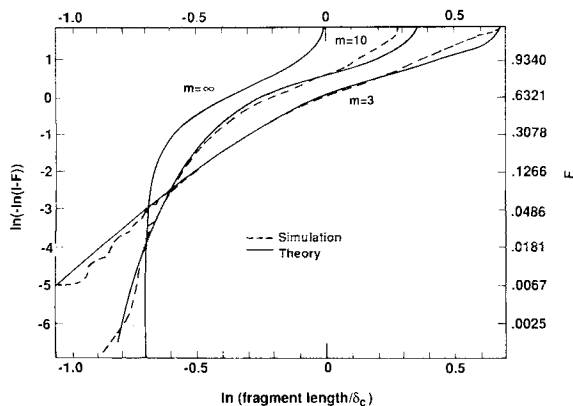


Fig. 3. Cumulant of the predicted fiber fragment probability distribution F versus fragment length x in the Weibull plot form of $\ln[-\ln(1 - F)]$ vs $\ln x$ for several Weibull moduli, with results obtained by computer simulations (see Ref. 9 for further details).

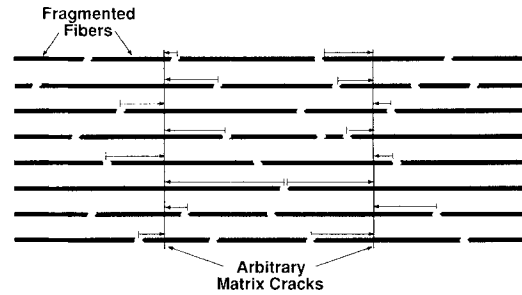


Fig. 4. Schematic determination of pullout lengths after complete fiber fragmentation. Pullout length is the shorter of the two pieces formed when the matrix crack intersects a fragment, as shown by the arrows.

of such a fragment along the fiber,

$$P_i(x) = \frac{x}{\langle x \rangle} P(x) \quad (10)$$

Having intersected a length x fragment, the pullout length is the shorter of the two pieces of the bisected fragment, since the shorter piece requires less force to pull out than the longer piece (see Fig. 4). Therefore, given a length x fragment, the distribution of possible pullout lengths $P_x(L)$ from this length fragment is

$$P_x(L) = \frac{2}{x} \quad 0 < L < \frac{x}{2} \quad (11a)$$

$$= 0 \quad \frac{x}{2} < L \quad (11b)$$

The total $P(L)$ for the composite is the sum over all fragment sizes x of the product $P_i(x)P_x(L)$,

$$P(L) = \int_0^\infty dx P_i(x)P_x(L) = \frac{2}{\langle x \rangle} \int_{2L}^\infty dx P(x) \quad (12)$$

$P(L)$ is shown in Fig. 5 for a range of m values. Equation (12) shows that all fragments longer than $2L$ can cause a pullout of L . For L much smaller than a typical fragment size, the probability is thus essentially independent of L , accounting for the flatness of $P(L)$ for $L \leq \delta_c/4$, since most fragments are greater than or equal to $\delta_c/2$ (see Fig. 3).

From $P(L)$, all the moments

$$\langle L^n \rangle = \int dL L^n P(L)$$

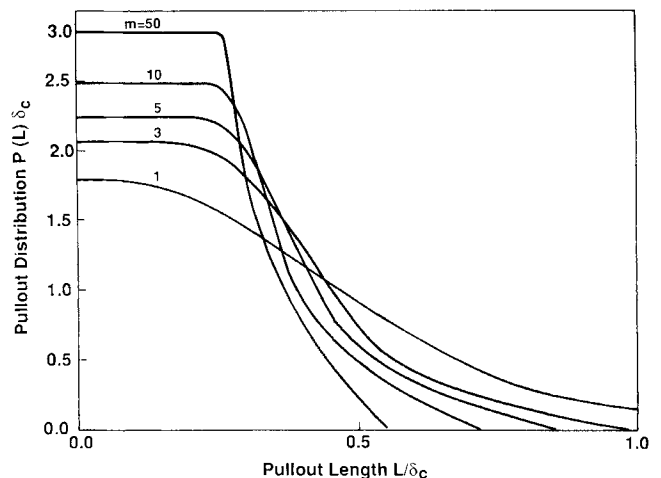


Fig. 5. Dimensionless pullout length distribution $P(L)\delta_c$ vs L/δ_c for a wide range of m . $m = 50$ distribution is almost the same as the asymptotic $m \rightarrow \infty$ distribution.

can be calculated. However, it is instructive to calculate the mean pullout length $\langle L \rangle$ more simply and physically as follows. For a fragment of size x , the average pullout length is

$$\langle L_x \rangle = \int_0^\infty dL L P_x(L) = \frac{x}{4} \quad (13)$$

i.e., the average size of the smaller of the two pieces of any bisected fragment is just 1/4 of the fragment length. Now averaging this result over all fragment sizes x , we obtain the mean pullout length in terms of the moments

$$\langle x^n \rangle = \int dx x^n P(x)$$

of the fragment distribution as

$$\langle L \rangle = \int_0^\infty dx \langle L_x \rangle P(x) = \frac{1}{4} \frac{\langle x^2 \rangle}{\langle x \rangle} \quad (14)$$

Introducing Eq. (3) for the moments $\langle x^2 \rangle$ and $\langle x \rangle$ then gives

$$\langle L \rangle = \frac{1}{4} \frac{\lambda_2(m)}{\lambda_1(m)} \delta_c \quad (15)$$

where $\lambda_2(m)/\lambda_1(m) = \langle x^2 \rangle / \delta_c \langle x \rangle$ is the dimensionless ratio of the second and first moments of $P(x)$. Equation (15) is one of the main results of this work: The average pullout length is proportional to δ_c . The result of Sutcu⁴ differs only in the m -dependent prefactor, with $\lambda_2(m)/\lambda_1(m)$ replaced by $\Gamma((m+2)/(m+1))$, as shown in Fig. 6 (Γ is the well-known gamma function). Sutcu's result overestimates the pullout lengths for $m \geq 7$ and underestimates them for $m \leq 6$ because of the neglect of multiple breaks along a single fiber.

The work of pullout can be shown to be proportional to $\langle L^2 \rangle$. However, W_p can be obtained most simply as follows. First, the work to pullout any L against the frictional "pressure" τ is $\pi r \tau L^2$. Hence, the average work to pull out a piece of a single fragment of length x is

$$W(x) = \int_0^\infty dL P_x(L) \pi r \tau L^2 = \frac{\pi r \tau}{12} x^2 \quad (16)$$

The work per area of the entire composite is then simply the average of $W(x)$ over all intersected fragment lengths x ,

$$W_p = \frac{f}{\pi r^2} \int_0^\infty dx \frac{\pi r \tau}{12} x^2 P(x) = \frac{1}{12} f \frac{\tau}{r} \frac{\langle x^3 \rangle}{\langle x \rangle} \quad (17)$$

By again introducing the key length δ_c and σ_c we obtain

$$W_p = \frac{1}{12} \frac{\lambda_3(m)}{\lambda_1(m)} f \sigma_c \delta_c \quad (18)$$

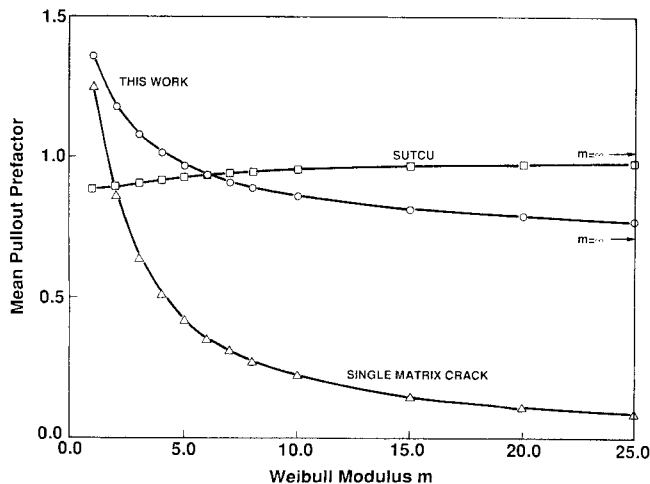


Fig. 6. m -dependent prefactor of the mean pullout length $\langle L \rangle$ for this work and that of Sutcu⁴ under multiple matrix cracking and for the single matrix crack case.

where $\lambda_3(m)/\lambda_1(m) = \langle x^3 \rangle / \delta_c^2 \langle x \rangle$ is the ratio of the dimensionless third moment of $P(x)$ to the first moment of $P(x)$. Equation (18) is the second main result of this paper: The work of pullout is proportional to $\sigma_c \delta_c$. Again, Sutcu's⁴ result differs only in the prefactor, with $\lambda_3(m)/\lambda_1(m)$ replaced by $\Gamma((m+3)/(m+1))$, as shown in Fig. 7.

Our main results of Eqs. (15) and (18) show that the pullout behavior is dominated by the characteristic gauge length δ_c , with relatively slowly varying m -dependent prefactors. Since both σ_c and δ_c increase with increasing σ_0 , higher fiber strengths always improve the pullout. However, although δ_c increases with increasing r and/or decreasing τ , the dependence of σ_c on r and τ depends on m . Thus, the dependence of W_p on r and τ varies with m nonmonotonically. In any case, accounting for multiple fiber breaks leads to important differences in magnitude in comparison to Sutcu⁴ (see Fig. 7), which may be important in determining the optimum parameters for overall composite performance (work of fracture and ultimate strength; see below). Our results also show that multiple matrix cracking is always preferable to single matrix cracking for pullout, and that the pullout prefactors are monotonic in m .

Both the present calculations and those of Sutcu⁴ predict finite pullout lengths in the limit $m \rightarrow \infty$. These results thus contradict the standard view that no pullout is possible in the limit $m \rightarrow \infty$.^{3,7} The argument in support of the standard view is that, as $m \rightarrow \infty$ (i.e., the fiber strength approaches a unique, gauge-length-independent value σ_0), fiber fracture always occurs in the matrix crack planes, and, hence, no pullout can occur. Thus, by eliminating from consideration the small but finite stress variations in the fibers due to the matrix cracks (compare Figs. 2(A) and (B)), we also eliminate the increasing preference for fracture in the matrix crack planes and thereby might erroneously predict finite pullouts as $m \rightarrow \infty$. However, although it is true that, as $m \rightarrow \infty$, fiber fracture occurs only in the matrix planes, not all fibers fracture in the same matrix plane. The underlying reason for this is that the slip lengths l_f are larger than the matrix crack spacing (see Fig. 1(D)), $l_f > l_m$, and, hence, a fracture in one matrix plane can induce fractures in other nearby matrix planes within l_f , and these secondary failures then prohibit failures in the original matrix plane. Therefore, only some fiber failures occur in any one plane, and the fractures in the remaining planes pull out through the matrix blocks. We discuss this more extensively in a subsequent paper,¹⁵ where we conclude that pullout on the order of $\langle L \rangle = \delta_c/4$ occurs for almost all values of m , and always for $m/N_f \leq 1$, where N_f is the actual number of fibers in the sample cross section. Thus, the results predicted here are at least qualitatively, if not quantitatively, correct in the large- m limit. For most practical cases,

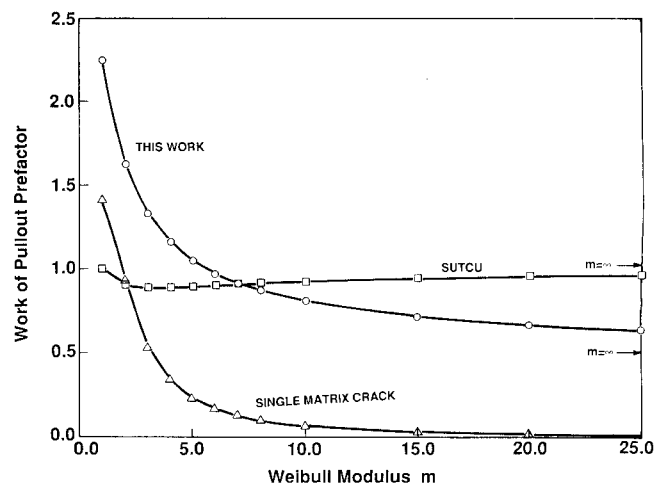


Fig. 7. m -dependent prefactor of the work of pullout W_p .

$m/N_f \leq 1$ holds, and our estimates of finite pullout are reasonable and physically motivated.

III. Ultimate Tensile Strength

The load-bearing capacity of the composite after matrix cracking is the same as that of the fibers in any matrix crack plane. Considering, then, a single matrix-crack plane at applied load σ , the average stress per fiber is σ/f . This load is partially carried by fibers with no breaks within $\pm l_f$ of the matrix crack and, hence, which cannot be pulled out at the present stress. The remainder of the load is carried by those fibers that are broken within a slip length of the crack plane. If we denote the stress carried by the unbroken fibers as T and the fraction of fibers broken within $\pm l_f$ by $q(l_f)$, then T and q must satisfy

$$\frac{\sigma}{f} = T(1 - q(l_f)) + \frac{2\tau}{r} \langle L(T) \rangle q(l_f) \quad (19)$$

The first term in Eq. (19) represents the load carried by the fraction $1 - q$ of unbroken fibers and the second term is the average load carried by the q broken fibers because of τ acting over the average pullout length $\langle L(T) \rangle$. Note that $\langle L(T) \rangle$ and l_f depend on the load T carried by intact regions of fiber; hence, $\langle L(T) \rangle$ is not the same as $\langle L \rangle$ in Eq. (16). Equation (19) can be simplified by recognizing that $l_f = rT/2\tau$, and, hence,

$$\frac{\sigma}{f} = T \left[1 - \left(1 - \frac{\langle L(T) \rangle}{l_f} \right) q(l_f) \right] \quad (20)$$

Since the pullout lengths are roughly proportional to l_f , the ratio $\langle L(T) \rangle/l_f$ is weakly dependent on T . σ_u is obtained by maximizing Eq. (20) with respect to T . The quantities $\langle L(T) \rangle$ and $q(l_f)$ are obtainable exactly from the single-fiber composite fragmentation theory evaluated at stress T prior to complete fragmentation, and therefore Eq. (20) can be maximized numerically to obtain σ_u .

Rather than conduct complete numerical solutions, it is instructive and accurate to make one approximation which yields very accurate results for σ_u and a subsequent approximation which yields accurate analytic results. The first approximation is to assume that, at the T maximizing Eq. (20), the probability of finding two breaks on the same fiber within $\pm l_f$ of the matrix crack is negligible. This is equivalent to assuming that, at T , the number of fiber fragments smaller than $2l_f$ is negligible. In this case, pullout occurs because of the matrix crack randomly intersecting a fragment within l_f of the end of the fragment. Being random, the average pullout length is then $\langle L(T) \rangle = l_f/2$, independent of T , and Eq. (20) further reduces to

$$\frac{\sigma}{f} = T \left(1 - \frac{1}{2} q(l_f) \right) \quad (21)$$

The error in σ_u associated with Eq. (21) is quite small, since almost all the fragments are $\geq 2l_f$ at the UTS. The second approximation to obtain analytic results is to approximate $q(l_f)$ by the fraction of breaks occurring in a gauge length $2l_f$, i.e., $q(l_f) = \Phi(2l_f, T)$ where Φ is given by Eq. (1). Again utilizing $l_f = rT/2\tau$, we find that σ/f depends only on T and that $\sigma_c = \tau\delta_c/r$ again appears:

$$\frac{\sigma}{f\sigma_c} = (T/\sigma_c) \left[1 - \frac{1}{2} (T/\sigma_c)^{m+1} \right] \quad (22)$$

Equation (22) is now easily maximized with respect to T to yield

$$\sigma_u = f\sigma_c \left(\frac{2}{m+2} \right)^{1/(m+1)} \frac{m+1}{m+2} \quad (23)$$

with the fraction failed $q = 2/(m+2)$ and $T/\sigma_c = [2/(m+2)]^{1/(m+1)}$ at this point. Equation (23) is the third main

result of this work: The UTS is directly proportional to the key stress σ_c . Figure 8 shows the ratio $\sigma_u/f\sigma_c$ vs m as predicted by Eq. (23) and by the very accurate Eq. (21); the analytic result underestimates σ_u by 7% at $m = 1$ but quickly approaches the accurate numerical result with increasing m . These results are expected to be similar to that from Sutcu's⁴ theory because q is small at the UTS, but Sutcu only presented results for a complete solution to Eq. (19) for one particular set of material parameters.

Note that, at low m , a nonnegligible portion of the load-bearing capacity of the composite is borne by broken fibers. On average, since $\langle L(T) \rangle/l_f \approx 1/2$, broken fibers carry one-half the load of unbroken fibers. If this contribution is neglected entirely ($\langle L(T) \rangle = 0$ in Eq. (20)), then the result for σ_u is reduced by the factor $2^{-1/(m+1)}$, which is appreciable at small m . The ratio $\sigma_u/f\sigma_c$, under neglect of the load carried by broken fibers, is also shown in Fig. 8.

Most previous estimates of the UTS have neglected not only the load carried by the broken fibers within $\pm l_f$ but have also adopted a "weakest-link" assumption by assuming that a fiber with a break anywhere within the entire sample gauge length L_s is incapable of carrying any load.^{10,11,13} In the limit that $2l_f \gg l_m$, as assumed here, the previous results can be shown to reduce to the form

$$\frac{\sigma_u}{f\sigma_c} = \left(\frac{\delta_c}{L_s} \right)^{1/m} \left(\frac{1}{em} \right)^{1/m} \quad (24)$$

where e is the natural logarithm base. The factor $(1/em)^{1/m}$ is the well-known dry-fiber-bundle failure result¹ also shown in Fig. 8, which only differs from the factor $[1/(m+2)]^{1/(m+1)}$ $[(m+1)/(m+2)]$ that we obtain by neglecting broken fibers because, in our case, the gauge length is varying during the test and therefore is not a fixed value as in the dry-fiber-bundle result. However, the difference in gauge length can be appreciable if $L_s \gg \delta_c$. The combination of neglecting the load carried by any broken fibers and making the weakest-link assumption is thus expected to lead to large underestimates of the UTS. Carrying the consequences of these assumptions further, if the load-bearing capacity of the fibers is negligible, there is negligible pullout work, and, if the weakest-link assumption holds, the pullout lengths are on the

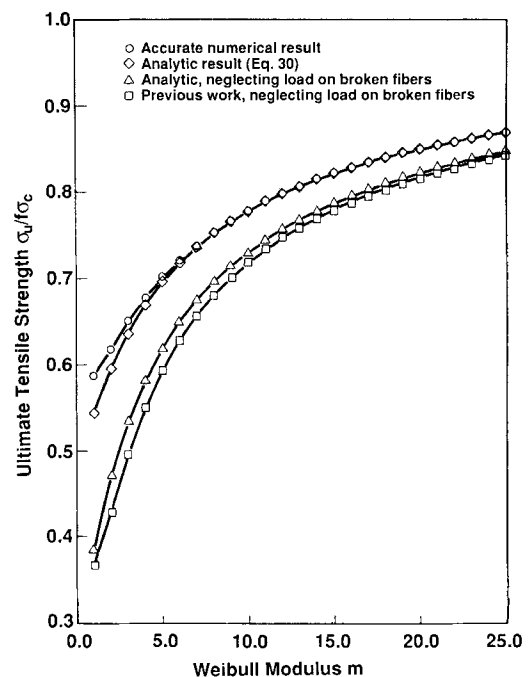


Fig. 8. Ultimate tensile strength $\sigma_u/f\sigma_c$ versus Weibull modulus m under various approximations.

order of L_c . Neither of these consequences is observed experimentally, raising doubts as to the validity of the assumptions leading to Eq. (24).

A recent theory for σ_u by Schwietert and Steif¹⁶ does account for the load-bearing capacity of broken fibers but also assumes that the relevant gauge length for failure is the matrix crack spacing. Since the fiber slip length is almost always larger than the matrix crack spacing, as discussed in Section II, the discussion of Schwietert and Steif does not appear applicable to CMCs; the neglect of "interactions" of fiber breaks between different matrix crack blocks is far too restrictive. The key idea of identifying a gauge length other than the sample gauge length as relevant to composite strength is contained in their work, however.

The composite strain after matrix cracking is essentially determined by the strain in the intact fibers since very little stress is carried by the matrix. Thus, the average composite strain is the average strain of the intact fibers at the matrix crack plane, $\epsilon = T/E_f$. The stress-strain curve for the composite *valid only up to failure* then follows directly from Eq. (22) as

$$\frac{\sigma}{\sigma_c} = \frac{\epsilon}{\epsilon_c} \left[1 - \frac{1}{2} \left(\frac{\epsilon}{\epsilon_c} \right)^{m+1} \right] \quad \epsilon \leq \epsilon_f \quad (25)$$

with $\epsilon_c = \sigma_c/E_f$ and failure strain $\epsilon_f = \epsilon_c[(2/(m+2))^{1/(m+1)}]$

IV. In Situ σ_c and m from Fracture-Mirror Data

The key parameters governing failure of CMCs have been shown to be δ_c , σ_c , and m . The use of ex situ fiber strength data on σ_0 and m at long gauge lengths $L_0 \gg \delta_c$ may, however, be inappropriate for calculating δ_c , σ_c , and m for the fibers in situ because of degradation of the fiber strengths during processing. Prewo¹² has shown that the strength of Nicalon fibers carefully extracted from a fully processed composite is reduced by about two-thirds relative to its original ex situ strength at the same gauge length. Therefore, it is extremely important to obtain in situ or postprocessing fiber strengths wherever possible. Fracture-mirror measurements,^{10,11} as described below, coupled with a knowledge of the evolution of fiber breaks in the composite may allow the in situ quantities σ_c and m to be determined directly.

The fracture surface of a broken fiber can exhibit a mirror-like region of radius a_m surrounding the underlying critical flaw of radius a_c . A semiempirical relationship between the radii a_m and a_c is given by¹⁷ $a_c/a_m \approx 0.22$ if $a_m \ll r$ and, thus, the deduction that the fiber failure strength is $S = K_f/3.5 a_m^{1/2}$, where K_f is the fracture toughness of the fiber. The use of fracture mirrors to obtain in situ fiber strengths of pulled-out fibers has recently been proposed by Cao *et al.*¹¹ as a means of assessing fiber degradation, and they find that the strengths S follow a Weibull-like behavior. Specifically, the cumulative probability of failure $G(S)$ at stress S obeys

$$G(S) = 1 - \exp[-(S/S^*)^{m^*}] \quad (26)$$

However, this distribution of failure stresses, characterized by mean S^* and Weibull modulus m^* , is *not* the same as the true fiber strength distribution characterized by σ_c and m . The reason that the in situ strength distribution from pulled-out fibers is different from the fiber strength distribution is because, when a fiber break does occur, the stress within $\pm l_f$ decreases irreversibly and the defects within $\pm l_f$ of the break can never fail under a subsequent loading. Each break thus screens out other potential breaks and the observed number of breaks versus stress differs from the number of underlying defects versus stress.

Our interpretation of the pullout lengths as due to an underlying single-fiber fragment distribution allows the relationship between (σ_c, m) and (S^*, m^*) to be calculated explicitly. For input values of σ_c and m , the predicted fraction of breaks

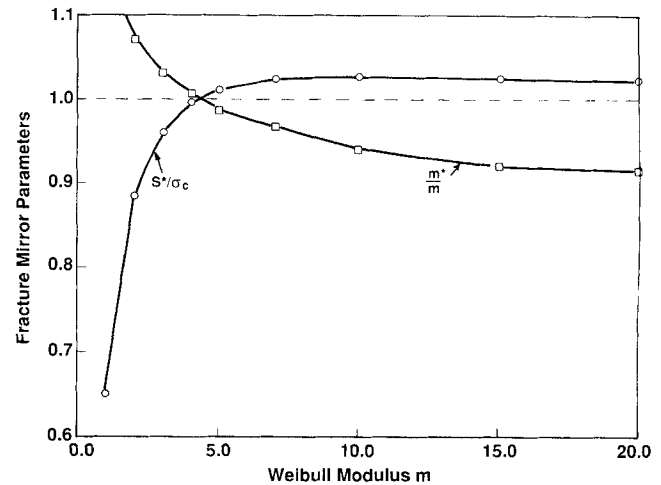


Fig. 9. Dependence of Weibull scale parameters (S^*, m^*) determined from fracture-mirror data on underlying parameters (σ_c, m) characterizing the in situ fiber strength statistics.

versus stress during tensile testing does approximately follow the Weibull form of Eq. (26).⁹ For each (σ_c, m) there is thus a unique (S^*, m^*) which best characterizes the fracture-mirror strength data, as shown in Fig. 9. In practice, we can determine (S^*, m^*) from the fracture mirrors of pulled-out fibers and then utilize Fig. 9 to derive the true (σ_c, m) describing the in situ fiber strengths at gauge length δ_c . This (σ_c, m) can then directly enter our expressions for $\langle L \rangle$, W_p , and σ_u to yield the predicted composite behavior. Note that, within the present theory, there should be no correlation between S and L for any particular fiber.

V. Applications of the Theory

Only a few sets of mechanical measurements on ceramic-matrix composites exist in the literature which provide the requisite in situ fiber strength data, and these measurements are only on the matrix cracking stress and UTS. There are no published data, to our knowledge, on measured pullout length distributions or work of fracture for samples tested in simple tension. Thus, a comparison of our complete theory to experiments is not possible at present; we are necessarily limited to a comparison of σ_u . Unfortunately σ_u is most susceptible to deviations from the theoretical predictions because of fibers failed in the crack wake or on processing and/or strain localization around one matrix crack plane. The predicted σ_u given by Eq. (23) is thus expected to be an upper bound.

Prewo¹² has investigated the failure of a number of Nicalon fiber/lithium aluminum silicate (LAS) glass matrix composites, with additional work on assessing the strength statistics of postprocessed fibers carefully extracted from composites similar to those tested. The general system parameters are shown in Table I for the LAS-II matrix, and the postprocessed fiber strength data are shown in Table II. A straightforward calculation of σ_c via Eq. (2b) and then of σ_u using Eq. (23) yields our theoretical predictions, also shown in Table II for the two values $\tau = 2$ MPa and $\tau = 3$ MPa esti-

Table I. Parameters for Nicalon/LAS CMC*

Parameter	Value
Radius, r	8 μ m
Fiber modulus, E_f	193 GPa
Matrix modulus, E_m	83 GPa
Matrix toughness, Γ_m	4×10^{-5} MPa \cdot m
Fiber volume fraction, f	≈ 0.45
Sliding resistance, τ	2–3 MPa

*Reference 12.

Table II. Strength Data for Nicalon Fibers and Nicalon/LAS-II Composites

Sample*	f	Fiber strength, σ_0 (MPa) [‡]	m	Ultimate strength (MPa)	
				Experimental	Theory [‡]
2369 (p)	0.46	1740	3.8	717–795	693,753
2369 (c)	0.46	1740	2.7	641–681	707,788
2376 (p)	0.44	1615	3.9	653–683	623,677
2376 (c)	0.44	1632	3.1	664–686	637,704

* (p) is as-pressed and (c) is sintered. [†]At $L_0 = 2.5$ cm. Prewo¹² quotes mean strength as 50% failure; our σ_0 is the stress at 63.2% failure, which is larger by $(\ln 2)^{-1/m}$. [‡] $\tau = 2.3$ MPa.

mated to be the range appropriate for these composites.^{4,11} Agreement between theory and experiment is quite good, especially considering the neglect of small effects, such as residual stresses, and the assumption of global load sharing. The one inconsistency, for samples 2369(c), has the theory too large by about 10%. In all cases the predicted average pullout is in the range of 1.5 to 2.5 mm, which is consistent with the experimental values.

Prewo¹² has found that the mean fiber strength (stress at 50% failure, or $\sigma_0(\ln 2)^{1/m}$ in the present notation) multiplied by f gives a fair account of the composite strength. In light of the present results, such agreement is largely fortuitous. The fact that the product of σ_c (which is higher than σ_0 because it is the strength at a smaller length $\delta_c < L_0$) and the “bundlelike” factor $[2/(m+2)]^{1/(m+1)}[(m+1)/(m+2)]$ (which is smaller than unity) yields a number in the vicinity of σ_0 in this case is coincidental. Had Prewo’s composites been longer and the fibers tested at the longer length to give a new σ_0 , we conjecture that the UTS would be unchanged nonetheless.

Cao *et al.*¹¹ have also performed an exhaustive study of the Nicalon fiber/glass matrix composite system, with variations in fiber-sliding resistance from material to material so as to probe more of the wide parameter space covered by theory. In particular, they have obtained fracture-mirror data, which we will utilize via Fig. 9, and have considered the effects of residual stresses, which we continue to neglect for simplicity. The system parameters quoted by Cao *et al.* for the fiber and matrix are as in Table I, again with fiber fraction here as $f = 0.45$.¹⁸ The fracture-mirror data and predicted UTSs for an LAS-III matrix (materials A and B), an aluminosilicate matrix (material C), and a soda–lime–glass matrix (material D) are all shown in Table III. In contrast to the agreement with the results of Prewo, our predictions of σ_u are systematically too large by 20% to 30%. There are several possible reasons for this discrepancy. First, since the sample gauge length used is only a few δ_c , multiple fractures along each fiber may be reduced, and σ_c may be closer to the measured S^* than suggested by Fig. 9; this would account for about 10% of the difference. Second, the quoted fiber fractions are approximate, and the actual values may be lower. The measured values of $\sigma_u = 550$ MPa are almost the same as that measured by Mah *et al.*¹⁹ on nominally identical samples, but with a measured fiber fraction of only $f = 0.40$; if the materials of Cao *et al.* are at $f = 0.40$, this accounts for another 10% of the deviation. These possibilities notwithstanding, recent measurements on materials nominally identical to A, B, and C, performed by Leckie *et al.*,²⁰ have yielded $\sigma_u = 790$ MPa, which is in excellent agreement with our original predictions of 750 MPa. The sensitivity of σ_u to processing and testing must be addressed carefully in future work.

VI. Discussion

We have presented a theory to predict the dependence of nearly all the important mechanical properties ($\langle L \rangle, W_p, \sigma_u$) on the material parameters $\tau, r, \sigma_0, L_0, m$, and f of ceramic-matrix composites which undergo multiple matrix cracking prior to composite failure. Under the assumption of global load transfer from broken to unbroken fibers, the theory considers each fiber as undergoing successive fragmentation with increasing stress in a manner identical to the fragmentation process which would occur in a tensile test of the same fiber embedded in a homogeneous large-failure-strain matrix. The known solution to the single-fiber composite fragmentation process is then directly applicable to the multifiber composite, and our results are valid when the typical fiber strengths are much larger than the matrix cracking stress. The main feature which emerges from this conceptual view of the CMC mechanical behavior is that there is a characteristic gauge length δ_c and a corresponding strength $\sigma_c = \tau\delta_c/r$ that govern the full dependence of $\langle L \rangle, W_p, W_b$, and σ_u on τ, r, σ_0, L_0 , and m , with slowly varying m -dependent numerical coefficients. The characteristic gauge length δ_c which controls all these properties is the generalization of Kelly’s critical length l_c to fibers with a statistical strength distribution ($m < \infty$). The associated in situ strength σ_c and m are obtainable directly from fracture-mirror data.

The close connection between δ_c and Kelly’s l_c shows that the pullout properties of a continuous CMC are very similar to those for a uniaxially aligned discontinuously reinforced material of the same fibers but of lengths on the scale of δ_c . However, a major difference lies in the UTS of these two types of materials. Since the fraction of failed fibers at the UTS is only $q \approx 2/(m+2)$, many of the fibers in the continuous composite carry the full load T . In the discontinuously reinforced composite no fiber carries the full load T , and, hence, the UTS must be considerably lower. The continuously reinforced material is thus preferable for the best overall composite performance.

The prediction of finite pullout as $m \rightarrow \infty$ under multiple matrix cracking, in contrast to the case of zero pullout for single matrix cracking, shows that high m are generally preferable. W_p does not necessarily decrease with increasing m , whereas σ_u does increase. Furthermore, the natural drive toward improving fiber strengths is expected to be accompanied by an increase in m , since eliminating the weakest types of defects both increases average strength and narrows the strength distribution. The desire to improve composite properties by using large m is thus in line with the desire for fiber improvement. However, high m may be undesirable for unbridged notch strength; therefore, an optimal m will depend on the prime material application.²¹

Since all the key composite properties are linked only by their dependence on δ_c and σ_c , a full set of measurements on a tensile-tested composite provides a very strict test of our present understanding of these uniaxially reinforced CMCs. Specifically, measurements of σ_{mc} and average matrix crack spacing provide initial information on the value of τ . Measurements of σ_u , the work of fracture, and the mean pullout length should all be related by a single choice of δ_c (and, hence, $\sigma_c = \tau\delta_c/r$) and m . Subsequent fracture-mirror measurements or data on extracted fibers provide another determination of σ_c and m . Deviations in the δ_c and/or m obtained from these different measurements can then provide considerable insight into shortcomings of the theory or evidence

Table III. Strength Data for Nicalon/Glass CMC Composites[†]

Sample	Fracture-mirror, S^* (GPa)/ m^*	In situ fiber strength, σ_c (GPa)/ m	σ_u (MPa)	
			Predicted	Measured
A, B, C	2.47/2.1	2.8/2.0	750	540 \pm 30
D	1.38/3.1	1.44/3.0	412	348 \pm 30

[†]Reference 11.

against the main assumption of global load transfer. Local load transfer would also lead to correlations in the pullout lengths of neighboring fibers, and additional (although time consuming) measurements of these correlations would contribute to our understanding of the load transfer process. Even within the context of global load sharing, the present theory also neglects the possibility of strain localization. Strain localization occurs if one particular matrix crack plane has more breaks within $\pm l_f$ than all others and, hence, a larger T . This then leads to enhanced breaking within $\pm l_f$, an increased T in this region, and, thus, a feedback process in which all the breaking and pullout is localized around the one or a few matrix crack planes. Strain localization could decrease the measured UTS and modify the pullout length distribution, but at present it is difficult to quantify this effect. In our subsequent paper¹⁵ dealing primarily with $m \rightarrow \infty$ limit, we will investigate the effects of strain localization further; our preliminary results indicate that strain localization has little effect on composite properties.

With a theory verified fully on one particular composite system, the theory can provide clear directions for the further optimization of the system by modifying "available" parameters such as fiber coating, fiber radius, and fiber fill fraction. The theory also shows the trade-offs between the optimization of various aspects of composite mechanical behavior, such as decreasing σ_u but increasing W_p with increasing r , or increasing σ_{mc} with increasing τ but with the difference $\sigma_u - \sigma_{mc}$ decreasing for large m . Knowledge of these trade-offs in quantitative terms implies control of the complete composite behavior and, hence, the possibility of designing functionally different composites for different applications from the same basic constituent fiber and matrix materials.

APPENDIX

Work of Fracture from Fiber Fracture

Strong fibers can make a contribution to the work of fracture of the composite over that of the pure matrix, even in the absence of pullout because of the work expended in elastically extending the fibers to failure. Although this contribution is expected to be small compared to W_p , it is useful to explicitly verify this expectation by calculation. The work of breaking W_b can be generally written as an integral over the crack-opening displacement u :⁵

$$W_b = 2f \int_0^{u^*} (1 - q)T du \quad (\text{A-1})$$

Here $1 - q$ is again the fraction of unfailed fibers at stress T and u^* is the "critical" crack-opening displacement. Marshall *et al.*⁷ have shown that u and T are related by

$$u = \frac{r}{4E_f\tau(1 + \xi)} T^2 \quad (\text{A-2})$$

where $\xi = fE_f/(1 - f)E_m$. If we change the variables in Eq. (A-1) from u to T and let the critical T^* be that at which $1 - q = 0$ (all fibers broken), then we have

$$W_b = f \frac{r}{\tau} \sigma_c^2 \frac{E_m(1 - f)}{E} \frac{\sigma_c}{E_f} \int_0^{T^*} (1 - q(y))y^2 dy \quad (\text{A-3})$$

where the introduction of the reference stress σ_c allows the integral to become nondimensional. Noting that Eq. (18) for

W_p may be rewritten as

$$W_p = \frac{fr}{\tau} \sigma_c^2 \frac{\lambda_3(m)}{12\lambda_1(m)}$$

we can express the ratio W_b/W_p as

$$\frac{W_b}{W_p} = \frac{\sigma_c}{E_f} \frac{12\lambda_1(m)E_m(1 - f)}{\lambda_3(m)E} \int_0^{\infty} (1 - q(y))y^2 dy \quad (\text{A-4})$$

The salient feature of Eq. (A-4) is that W_b/W_p is basically proportional to the characteristic failure strain (σ_c/E_f) of the fibers, which is $\ll 1$. The dimensionless integral varies only between 0.3 and 0.5 so that the combination of other terms in Eq. (A-4) is typically ≤ 0.1 . Explicit results for the Nicalon/LAS systems discussed in Section V yield $W_b/W_p \approx 0.03$. Hence, this contribution to the work of fracture can generally be neglected.

References

1. A. Kelly and N. H. MacMillan, *Strong Solids*, 3d ed. Clarendon Press, Oxford, U.K., 1986.
2. J. Aveston, G. A. Cooper, and A. Kelly, "Single and Multiple Fracture: The Properties of Fiber Composites," pp. 15-24 in *The Properties of Fibre Composites*, Conference Proceedings, National Physical Laboratory (Guildford, U.K.). IPC Science and Technology Press, Ltd., Teddington, U.K., 1971.
3. For a recent review see A. G. Evans and D. B. Marshall, "The Mechanical Behavior of Ceramic-Matrix Composites," *Acta Metall.*, **37**, 2567-83 (1989).
4. M. Suteu, "Weibull Statistics Applied to Fiber Failure in Ceramic Composites and Work of Fracture," *Acta Metall.*, **37**, 651-61 (1989).
5. M. D. Thouless and A. G. Evans, "Effects of Pullout on the Mechanical Properties of Ceramic-Matrix Composites," *Acta Metall.*, **36**, 517-22 (1988).
6. B. Budiansky, J. W. Hutchinson, and A. G. Evans, "Matrix Fracture in Fiber-Reinforced Ceramics," *J. Mech. Phys. Solids*, **34**, 167-89 (1986).
7. D. B. Marshall, B. N. Cox, and A. G. Evans, "The Mechanics of Matrix Cracking in Brittle-Matrix Composites," *Acta Metall.*, **33**, 2013-21 (1985).
8. D. B. Marshall and B. N. Cox, "Tensile Fracture of Brittle-Matrix Composites: Influence of Fiber Strength," *Acta Metall.*, **35**, 2607-19 (1987).
9. (a) W. A. Curtin, "Fiber Fragmentation in a Single-Filament Composite," *Appl. Phys. Lett.*, **58**, 1155-57 (1991). (b) W. A. Curtin, *J. Mater. Sci.*, **26** (1991).
10. (a) M. D. Thouless, O. Sbaizero, L. S. Sigl, and A. G. Evans, "Effect of Interface Mechanical Properties on Pullout in a SiC-Fiber-Reinforced Lithium Aluminum Silicate Glass-Ceramic," *J. Am. Ceram. Soc.*, **72**, 525-32 (1989). (b) M. D. Thouless, O. Sbaizero, E. Bischoff, and E. Y. Luh, "The Influence of Heat Treatment Upon Fiber Pullout in a Ceramic Composite," *Mater. Res. Soc. Symp. Proc.*, **120**, 333-39 (1988).
11. H. C. Cao, O. Sbaizero, M. Rühle, A. G. Evans, D. B. Marshall, and J. J. Brennan, "Effect of Interfaces on the Properties of Fiber-Reinforced Ceramics," *J. Am. Ceram. Soc.*, **73**, 1691-99 (1990).
12. (a) K. Prewé, "Tension and Flexural Strength of Silicon Carbide Fibre-Reinforced Glass-Ceramics," *J. Mater. Sci.*, **21**, 3590-600 (1986). (b) K. Prewé, "Advanced Characterization of SiC-Fiber-Reinforced Glass-Ceramic Matrix Composites," Interim Rept. R83-915939-1 on Office of Naval Research Contract N00014-81-C-0571, 1983.
13. H. Cao and M. D. Thouless, "Tensile Tests of Ceramic-Matrix Composites: Theory and Experiment," *J. Am. Ceram. Soc.*, **73**, 2091-94 (1990).
14. A. C. Kimber and J. G. Keer, "On the Theoretical Average Crack Spacing in Brittle Matrix Composites Containing Continuous Aligned Fibers," *J. Mater. Sci. Lett.*, **1**, 353-54 (1982).
15. W. A. Curtin, submitted to *J. Mech. Phys. Solids*.
16. H. R. Schwieter and P. S. Steif, "A Theory for the Ultimate Strength of a Brittle-Matrix Composite," *J. Mech. Phys. Solids*, **38**, 325-43 (1990).
17. R. W. Rice, *Treatise on Materials Science and Technology*, Vol. II; p. 199. Academic Press, New York, 1978.
18. John J. Brennan; private communication.
19. T. Mah, M. G. Mendiratta, A. P. Katz, R. Ruh, and K. S. Mazdiyasn, "Room-Temperature Mechanical Behavior of Fiber-Reinforced Ceramic-Matrix Composites," *J. Am. Ceram. Soc.*, **68**, C-27-C-30 (1985).
20. F. Leckie; private communication.
21. B. Budianski, URI Winter Study Group, University of California, Santa Barbara, CA, Jan. 1991. □